

---

**Effect of seawater salinity on pore-size distribution on a poly(styrene)-based resin and its adsorption of diarrhetic shellfish toxins**Fan Lin<sup>1</sup>, Sun Geng<sup>1</sup>, Qiu Jiangbing<sup>1</sup>, Ma Qimin<sup>1,2</sup>, Hess Philipp<sup>3</sup>, Li Aifeng<sup>1,2,\*</sup><sup>1</sup> College of Environmental Science and Engineering, Ocean University of China, Qingdao 266100, China<sup>2</sup> Key Laboratory of Marine Environment and Ecology, Ocean University of China, Ministry of Education, Qingdao 266100, China<sup>3</sup> Ifremer, Laboratoire Phycotoxines, 44311 Nantes, France\* Corresponding author : Aifeng Li, tel.: +86 532 66781935 ; email address : [lafouc@ouc.edu.cn](mailto:lafouc@ouc.edu.cn)

---

**Abstract :**

In the present study, okadaic acid (OA) and dinophysistoxin-1 (DTX1) were spiked into artificial seawater at low, medium and high estuarine salinities (9‰, 13.5‰ and 27‰). Passive samplers (HP20 resin) used for solid phase adsorption toxin tracking (SPATT) technology were exposed in these seawaters for 12-h periods. Adsorption curves well fitted a pseudo-secondary kinetics model. The highest initial sorption rates of both toxins occurred in the seawater of medium salinity, followed by seawater of low and high estuarine salinity. Pore volumes of micropores (< 2 nm) and small mesopores (2 nm < diameter < 10 nm) of HP20 resin decreased after adsorption of toxins in seawater at high and low salinity but not in seawater at medium salinity, which demonstrated that the toxin molecules entered into micropores and mesopores (below 10 nm in size) in seawaters of high and low salinity. More toxin or other matrix agglomerates were displayed on the surface of resin deployed in the seawater of medium salinity. Taking into consideration the pore-size distribution and surface images, it appears that intra-particle diffusion governs toxin adsorption in seawater at high salinity while film diffusion mainly controls the adsorption process in seawater at medium salinity. This is the first study to confirm that molecules of OA and DTX1 are able to enter into micropores (< 2 nm) and small mesopores (2 - 10 nm) of HP20 resin in estuarine seawater with high salinity (~27 ‰).

**Highlights**

► HP20 resin bags were deployed in three artificial seawaters at different salinity. ► Dynamic adsorption behaviour of OA and DTX1 by these SPATT bags was explored. ► The highest initial sorption rate of toxins occurred in seawater at medium salinity. ► Resin pores below 10 nm in size governed adsorption in natural seawater. ► Toxins were retained by pores in seawaters at high and low salinity.

**Keywords :** Diarrhetic shellfish toxins (DST), Solid phase adsorption toxin tracking (SPATT), HP20 resin, Salinity, Pore-size distribution, Pseudo-secondary kinetics equation

## 44 **1. Introduction**

45 Micro-algal toxins potentially threaten mariculture industry and ecosystem health  
46 as toxic algal blooms occur frequently and globally in coastal waters [1, 2]. Based on  
47 their chemical structures, these micro-algal toxins are classified into total eight groups  
48 including the okadaic acid (OA), azaspiracid (AZA), yessotoxin (YTX), pectenotoxin  
49 (PTX), brevetoxin, cyclic imine, saxitoxin (STX), and domoic acid (DA) groups.  
50 They can be accumulated and transferred along food webs of marine ecosystems  
51 including cultivated shellfish [3-5]. Therefore, poisoning events and victims  
52 frequently occurred due to consumption of contaminated seafood [6-8]. For example,  
53 diarrhetic shellfish poisoning (DSP) as a familiar poisoning event is related to  
54 OA-group toxins, including OA and its derivatives dinophysistoxin-1 (DTX1) and  
55 epimer DTX2, accumulated by crabs, mussels, etc [9-12]. Although no victims were  
56 recorded by DSP events, a link was hypothesized between exposure to OA-group  
57 toxins and tumor enhancement [13-14]. Thus, it is very important to monitor and  
58 forecast the pollution of micro-algal toxins in mariculture zones in order to protect  
59 seafood safety and consumer health.

60 A technology referred to as Solid Phase Adsorption Toxin Tracking (SPATT) was  
61 developed to monitor the occurrence of toxic algal blooms and shellfish  
62 contamination events in seawater using porous synthetic resin [15]. Various  
63 micro-algal toxins were tentatively monitored using the SPATT method for adsorption  
64 in the laboratory or in the field [16-20]. The SPATT technology has been shown to  
65 provide reliable, sensitive, time-integrated sampling of various micro-algal toxins to

66 monitor the occurrence of toxic algal bloom events [21]. Comparative results for  
67 several different adsorbents showed that the resin DIAION<sup>®</sup>HP20 has greater  
68 adsorption quantity and higher desorption rate of lipophilic toxins [15, 16]. The key  
69 role played by the pore-size distribution, especially micropores of resin, for OA-group  
70 toxins was hypothesized in our previous study [22]. Utility of SPATT bags packaged  
71 by HP20 resin was also demonstrated to successfully monitor microcystins in  
72 freshwater [23]. Presently, the range of sorbents for passive sampling of micro-algal  
73 toxins was extended and assessed in laboratory and field studies [24]. However, the  
74 relationship between the quantity obtained by SPATT bags and toxin content  
75 accumulated by shellfish has still not been successfully modelled until now, although  
76 some efforts into this direction have been made [25]. Also, knowledge on the  
77 adsorption mechanism of toxins by resins and the effect of salinity on the adsorption  
78 process is still limited. In the present study, the dynamic adsorption of OA and DTX1  
79 toxins by HP20 resin in artificial seawater at different salinity was simulated in  
80 laboratory. The pore-size distribution and surface image of resins before and after  
81 adsorption toxins were explored to discuss the effect of salt matrix on the dynamic  
82 adsorption of toxins by HP20 resin.

## 83 **2. Materials and methods**

### 84 *2.1. Chemicals*

85 All reagents and solvents used in the study were HPLC grade. Acetonitrile and  
86 methanol were purchased from Merck Ltd. (Whitehouse Station, NJ, USA). Formic  
87 acid (FA) and ammonium formate (AF) were purchased from Fisher Scientific (Fair

88 Lawn, NJ, USA). Standard OA and DTX1 were purchased from the Certified  
89 Reference Materials Program (CRMP) of the National Research Council of Canada  
90 (Halifax, NS, Canada) and Wako Pure Chemical Industries, Ltd. (Osaka, Japan),  
91 respectively. Pure water was obtained from a MilliQ water purification system  
92 (Millipore Ltd., Bedford, MA, USA) to  $18.2 \text{ M}\Omega \text{ cm}^{-1}$  quality or better.

### 93 2.2. Adsorbent resin

94 DIAION<sup>®</sup>HP20 was purchased From the Mitsubishi Chemical Corporation  
95 (Tokyo, Japan). It is an aromatic type adsorbent based on a cross-linked polystyrene  
96 matrix. The manufacturer stated that particles of HP20 resin are 250-600  $\mu\text{m}$  (more  
97 than 90% particles  $> 250 \mu\text{m}$ ).

### 98 2.3. Dynamic adsorption of OA and DTX1 by HP20 resin in artificial seawaters

99 SPATT bags were made of polyester mesh, 40 mm  $\times$  40 mm, and were packed  
100 with 3.0 g of dry HP20 resin. They were immersed in methanol for 48 h to activate  
101 the HP20 resin. Then they were washed three times using bulk Milli-Q water before  
102 storage in pure water for use.

103 According to the manufacturer's statement, 31 g sea salt was dissolved in 1 L of  
104 pure water to simulate nature seawater with the content of NaCl,  $\text{MgSO}_4 \cdot 7\text{H}_2\text{O}$ ,  
105  $\text{MgCl}_2 \cdot 6\text{H}_2\text{O}$ ,  $\text{CaCl}_2 \cdot \text{H}_2\text{O}$  and KCl at  $65.0 \pm 5.0$ ,  $15.0 \pm 2.0$ ,  $12.0 \pm 2.0$ ,  $4.0 \pm 1.0$ , and  
106  $1.5 \pm 1.4$ , respectively. In this study, 31 g, 15.5 g and 10.3 g sea salt were dissolved in  
107 1 L of pure water to make the artificial seawater at high, medium, and low salinity,  
108 respectively. Salinity of the artificial seawater at high salinity was approximately 27‰,  
109 which was lower than that of normal natural seawater. Purified extracts of OA and

110 DTX1 toxins (10 mL) through solid-phase extraction (SPE) were dissolved in  
111 different salinity matrix and were added into the corresponding artificial seawater.  
112 The initial concentrations of OA and DTX1 toxins in the adsorption system were 2.70  
113 and 3.92 ng/mL, respectively. Three SPATT bags of HP20 resin were separately put  
114 into the different artificial seawater strengths using a weight to hold them in the  
115 middle of the container. The adsorption system was stirred continuously at 145 rpm  
116 by a magnetic stirring apparatus at  $25 \pm 1^\circ\text{C}$  in order to make toxins well-distributed.

117 Sampling time point was set at 0, 10, 20, 30, 45, 60, 90, 120, 240, 480 and 720  
118 min. Triplicate of 1.5 mL seawater was taken from the adsorption system at every  
119 sampling time point, respectively. These samples were purified by the Oasis<sup>®</sup>HLB  
120 SPE cartridge (3cc, 60mg). 2 mL of methanol and 2 mL of water was successively  
121 used to activate and equilibrate the cartridges, respectively, before loading 1.5 mL of  
122 samples. Aliquots (2 mL) of 5% methanol (methanol/water, 5/95, v/v) were used to  
123 wash and methanol (2 mL) was used to elute toxins. Finally, the eluate was dried by  
124 nitrogen gas and reconstituted in 1.5 mL of methanol. Then, the samples were filtered  
125 by 0.22  $\mu\text{m}$  organic membrane and analyzed using LC-MS/MS. Meanwhile, the same  
126 SPATT bags were deployed in different artificial seawater without micro-algal toxins  
127 in a 1 L flask as blank control experiment.

#### 128 *2.4. LC-MS/MS analysis for OA and DTXI*

129 An Agilent 6430 tandem quadrupole mass spectrometer equipped with an  
130 Agilent 1290 HPLC (Palo Alta, CA, USA) using an ESI interface was used to analyze  
131 all samples here. Chromatographic separation was achieved on a  $50 \times 2.1$  mm i.d.,

132 3  $\mu\text{m}$ , Luna C18 column (Phenomenex) maintained at 35°C. The mobile phase  
133 gradient was composed by solvent A (water) and solvent B (95% acetonitrile), each  
134 containing 50 mM formic acid and 2 mM ammonium formate. A gradient was run  
135 from 25% to 100% B over 7 min, holding for 3 min and back to 25% B to  
136 re-equilibration for 2 min for the next run. Flow rate was set at 300  $\mu\text{L}/\text{min}$  and the  
137 injection volume was 5  $\mu\text{L}$ . MS detection was carried out with positive ionization  
138 mode. Multiple reaction monitoring (MRM) acquisition mode was used for qualitative  
139 and quantitative analysis for OA ( $m/z$  827.5  $\rightarrow$  809.4 / 791.3 / 723.4) and DTX1 ( $m/z$   
140 841.5  $\rightarrow$  823.5 / 805.5 / 737.4).

#### 141 *2.5. Measure for surface area and porosity of resin*

142 HP20 resin was taken out from the SPATT bag after exposure in the adsorption  
143 experiments. The resin was freeze-dried using a lyophilizer at -40°C. Pore volume and  
144 pore-size distribution were determined by a gas sorption system (Micrometrics,  
145 ASAP<sup>®</sup> 2020, USA) using nitrogen as adsorbate. About 100 mg of resin was degassed  
146 at 105°C until the pressure increase rate was lower than 1.3 Pa/min within a 0.5-min  
147 test interval. Helium was used as a backfill gas. In total, 106 adsorption points and 54  
148 desorption points were collected from  $5.63 \times 10^{-7}$  to 0.995 P/P0.

#### 149 *2.6. Scanning electron microscopy for HP20 resin*

150 The surface texture of HP20 resin in different artificial seawater spiked with or  
151 without OA and DTX1 toxins were characterized by a scanning electron microscope  
152 (SEM) (Hitachi, S-4800, Japan). All resin samples were freeze-dried under vacuum  
153 and then were fixed on aluminum stubs and coated with gold before observation using

154 SEM.

### 155 **3. Results and Discussion**

156 *3.1. Dynamic adsorption behavior of OA and DTX1 toxins by HP20 resin in different*  
157 *artificial seawater*

158 Chemical structures of OA and DTX1 toxins are shown in Fig. 1. These  
159 polyether toxins can be dissolved in seawater due to salt matrix but not in freshwater  
160 because of their hydrophobic property. It is very difficult to arrange duplicate SPATT  
161 bags for each sampling time point because of limits of toxins and experimental space.  
162 The dynamic adsorption quantity of toxins on SPATT bags was calculated by the  
163 concentration discrepancy between two adjacent samplings from seawater. The  
164 chromatograms of OA and DTX1 toxins acquired by different transitions using  
165 LC-MS/MS are shown in Fig. 2. Retention times of OA and DTX1 toxins were 5.0  
166 and 6.0 min, respectively, under these chromatographic conditions. The  
167 chromatograms demonstrated that no obvious matrix interferences were found due to  
168 potential remaining salt matrix in the seawater samples purified by SPE cartridges.  
169 Limits of quantification (LOQ, signal / noise = 10) of the LC-MS/MS method for  
170 standard OA and DTX1 were measured as 0.23 and 0.07 ng/mL (injection volume 5  
171  $\mu$ L), respectively, using the S/N values of the lowest transitions of OA (827.5  $\rightarrow$   
172 791.3) and DTX1 (841.5  $\rightarrow$  805.5).

173 Dynamic adsorption curves of OA and DTX1 toxins adsorbed by HP20 resin in  
174 different artificial seawater are shown in Fig. 3. The curves showed that OA and  
175 DTX1 toxins could be adsorbed fast by HP20 resin in three different artificial

176 seawaters. The adsorption curves were close to linear type in the first 90-min time  
177 period. Relatively, the adsorption rates of OA and DTX1 toxins were the slowest in  
178 seawater at high salinity over the first 120-min; then they exceeded those in the  
179 seawater of low salinity after this period. Totally the adsorption rates of toxins in the  
180 seawater of medium salinity were the fastest in whole exposure period and there were  
181 no detectable toxins in this seawater after 480-min adsorption. The adsorption curves  
182 were simulated by five different dynamic adsorption models including the Elovich  
183 equation, double constant equation, parabolic diffusion equation, first-order kinetics  
184 equation and pseudo-secondary kinetics equation. The determination coefficient ( $R^2$ )  
185 demonstrated that the dynamic adsorption curves could be well fitted by the  
186 pseudo-secondary kinetics equation (Table 1). Values of  $R^2$  fitted by the  
187 pseudo-secondary kinetics equation decreased with the salinity in three different  
188 artificial seawaters, which demonstrated that the salinity of seawater slightly reduced  
189 the fit quality of the model.

190 Initial sorption rate  $h$  (ng/(g·min)) and equilibrium sorption quantity  $Q_e$  (ng/g)  
191 could be calculated using the pseudo-secondary kinetics equation using  $h= 1/a$  and  
192  $Q_e= 1/b$ [26]. The highest initial sorption rate occurred in the artificial seawater at  
193 medium salinity, followed by the treatment with low and high salinity (Table 2). This  
194 discrepancy showed that the salt matrix effectively reduced the initial sorption rates of  
195 OA and DTX1 toxins by HP20 resin. The initial sorption rate of OA was also less  
196 than that of DTX1 in three different artificial seawaters, which had been reported and  
197 explained by the extra methyl group of DTX1 in our previous study [22]. Average

198 linear sorption rates of OA and DTX1 toxins by HP20 resin were also directly  
199 calculated using the adsorption quantity divided by time period (Fig. 4). Average  
200 adsorption rates of OA and DTX1 in the seawater of low salinity slightly exceeded  
201 that in seawater of medium salinity in the early 10-min period. After this period the  
202 average adsorption rates in artificial seawater of medium salinity were the fastest,  
203 followed by the treatments of low and high salinity. This discrepancy of average  
204 linear adsorption rates also demonstrated that the salinity of seawater affected the  
205 dynamic adsorption behavior of lipophilic toxins by HP20 resin. Meanwhile, the  
206 average adsorption rates of OA in different seawater salinities were lower than those  
207 of DTX1 due to the difference of chemical structure. However, the equilibrium  
208 sorption quantities of OA and DTX1 toxins calculated by the pseudo-secondary  
209 kinetics equation increased with the salinity in three different artificial seawaters  
210 although the experimental sorption quantities were similar in all treatments (Table 2).

211 The concentrations of OA (2.70ng/mL) and DTX1 (3.92 ng/mL) used in this  
212 study were several hundreds of times higher than the dissolved OA concentration  
213 ranging from 4.24 to 9.64 ng/L in coastal seawater of Qingdao City, China [27].  
214 Theoretically the experimental quantities of OA and DTX1 were 900 and 1307 ng/g  
215 resin, respectively, if the toxins spiked into seawater were completely adsorbed by  
216 resin in the whole experimental period. The adsorption percentage of OA and DTX1  
217 spiked into three different seawaters was over 96% and 98%, respectively, when the  
218 adsorption experiment was finished in the study. These high percentages demonstrated  
219 that OA and DTX1 toxins were almost completely adsorbed by SPATT bags in the

220 experimental period. Therefore, the calculated equilibrium sorption quantities of OA  
221 and DTX1 in the artificial seawater increased with salinity because the salinity  
222 reduced the fit of the equation for adsorption. This point has been demonstrated by the  
223 values of determination coefficient  $R^2$ . Totally, the dynamic adsorption process could  
224 be well fitted by the pseudo-secondary kinetics equation which suggests that either  
225 film diffusion or intra-particle diffusion controls the overall rate of adsorption [26].  
226 Usually the dynamic adsorption process simultaneously depends on the large specific  
227 surface area and small size pores in the adsorbent. It means that the film diffusion  
228 governs adsorption process if the specific surface area plays dominant role; reversely  
229 it means the intra-particle diffusion governs the adsorption process. The intra-particle  
230 diffusion was hypothesized to govern the capacity and equilibration rate of toxin  
231 adsorption by HP20 resin in seawater of micro-algal cultures [16]. The important  
232 roles caused by micropores (< 2 nm) of HP20 resin in 90% methanol solution were  
233 also suggested in our previous study [22]. The dynamic adsorption behaviors of OA  
234 and DTX1 toxins by HP20 resin in different seawaters also comply with this rule in  
235 this study.

### 236 3.2. *Change of pore-size distribution of HP20 resin after adsorption for toxins*

237 In order to explore the mechanism by which salt affects the dynamic adsorption  
238 of toxins by resin, the pore-size distribution of HP20 resin deployed in seawater with  
239 or without OA/DTX1 toxins was characterized. Results showed that no obvious  
240 change of the pore volumes of size between 10-20 nm was found in HP20 resin  
241 deployed in three different seawaters with or without toxins (Fig. 5). However, the

242 pore volumes of micropores (diameter  $< 2$  nm) and small mesopores ( $2$  nm  $<$  diameter  
243  $< 10$  nm) decreased after toxins were adsorbed onto HP20 resin in the artificial  
244 seawaters at high salinity and low salinity, which demonstrated that toxin molecules  
245 entered into these small size pores. Inconsistently, the pore volumes of micropores did  
246 not change whether the resin adsorbed toxins or not, and the pore volumes of small  
247 mesopores ( $2 - 10$  nm) also did not change obviously and consistently in the artificial  
248 seawater at medium salinity. This phenomenon testified that the toxin molecules did  
249 not enter into the micropores and small mesopores ( $2 - 10$  nm) in the seawater of  
250 medium salinity. Interestingly, the pore volumes of micropores or mesopores ( $2 - 10$   
251 nm) of HP20 resin deployed in the artificial seawater of high salinity without toxins  
252 were higher than those in the artificial seawater of low salinity without toxins, which  
253 showed that solely the salt matrix of seawater also changed the pore size distribution  
254 of resin. Possibly, salt matrix would reconstruct these pores in some big pores of  
255 HP20 resin. The largest BET surface area of HP20 resin before adsorption toxins  
256 occurred in the seawater at high salinity, followed by the treatments of low and  
257 medium salinity (Table 3), which demonstrated that the salt matrix changed the  
258 surface area of resin. Consistently, the surface areas of resins decreased after they  
259 adsorbed toxins in three different seawaters. However, the average pore volume of  
260 resin deployed in the seawater at medium salinity increased after it adsorbed toxins,  
261 which also demonstrated that toxin molecules did not enter into these pores of resin.  
262 Therefore, the HP20 resin deployed in the seawater at medium salinity displayed the  
263 highest initial sorption rate because only film diffusion governed the adsorption

264 process.

265 In order to testify the discrepancy of adsorption behavior in different seawaters,  
266 the surface images of resin deployed in artificial seawaters were characterized by  
267 SEM. Results showed that the surface of resins deployed in three different seawaters  
268 without toxins were very clean (Fig. 6), which demonstrated that the salt matrix did  
269 not change resin surface. Some agglomerates emerged on the surface of resins  
270 exposed to algal extracts in seawaters of medium and low salinity, but not on the  
271 surface of resin adsorbed toxins in the seawater of high salinity (Fig. 6). More  
272 agglomerates occurred on the surface of resin deployed in the seawater at medium  
273 salinity comparatively to the seawater at low salinity. To our knowledge we could not  
274 explain the occurrence of agglomerates on the surface of resin deployed in the low  
275 salinity seawater. However, the SEM results testified that the toxins were mainly  
276 adsorbed onto the surface of resin deployed in the seawater at medium salinity  
277 (~13.5‰), which could explain the highest initial sorption rate due to the film  
278 diffusion related with surface adsorption.

279 Based on the findings of this study, it could be safely concluded that the  
280 intra-particle diffusion governs the adsorption process of HP20 resin for toxins in  
281 estuarine seawater with high salinity while film diffusion controls the adsorption  
282 process in seawater at medium salinity (~13.5‰). Also, the adsorption process of  
283 HP20 resin for toxins is dependent on both film diffusion and intra-particle diffusion  
284 in seawater of low salinity (~9‰). The different adsorption mechanisms for HP20  
285 resin in seawaters with different salinity suggest that the adsorption behavior of toxins

286 by SPATT deployments in estuaries with low salinity should be different to those in  
287 natural seawater.

#### 288 **4. Conclusions**

289 In this study, purified extract containing OA and DTX1 toxins from  
290 *Prorocentrum lima* was spiked into three artificial seawaters at different salinity (27‰,  
291 13.5‰ and 9‰) and SPATT samplers of HP20 resin were deployed in these seawaters  
292 for 720-min exposure. Adsorption curves of toxins in seawater of three different  
293 salinities well fitted the pseudo-secondary kinetics equation. However, the pore-size  
294 distribution and specific surface area of HP20 resins deployed in seawater with or  
295 without toxins were affected and not linearly related to the salinity of seawater.  
296 According to the findings of this study, it is confirmed that the molecules of OA and  
297 DTX1 are able to enter into the micropores and small mesopores (2 - 10 nm) of HP20  
298 resin in estuarine seawater at high salinity (~27‰). The intra-particle diffusion  
299 governs the adsorption process of HP20 resin for toxins in seawater with high salinity  
300 (~27‰), while film diffusion controls the adsorption process in seawater at medium  
301 salinity (~13.5‰). Further studies should clarify whether the effect of salinity on  
302 adsorption kinetics is sufficiently significant at the naturally low concentrations of  
303 toxins in seawater to play a role during daily or weekly monitoring.

#### 304 **Supplementary materials**

305 Extraction and purification methods for OA and DTX1 toxins could be found in  
306 the supplementary file.

#### 307 **Acknowledgement**

308           This work was funded by the Administration of Quality Supervision, Inspection  
309   and Quarantine, People's Republic of China (201310141), and the National Natural  
310   Science Foundation of China (41276103).

311   **Conflict of interest statement**

312           All authors declare that there are no conflicts of interest.

Accepted Manuscript

313 **References**

- 314 [1] L. Botes, A.J. Smit, P.A. Cook, The potential threat of algal blooms to the abalone  
315 (*Haliotis midae*) mariculture industry situated around the South African coast,  
316 Harmful Algae 2 (2003) 247-259.
- 317 [2] T.G. Park, W.A. Lim, Y.T. Park, C.K. Lee, H.J. Jeong, Economic impact,  
318 management and mitigation of red tides in Korea, Harmful Algae 30S1 (2013)  
319 S131-S143.
- 320 [3] L.F. Leandro, G.J. Teegarden, P.B. Roth, Z. Wang, G.J. Doucette, The copepod  
321 *Calanus finmarchicus*: A potential vector for trophic transfer of the marine algal  
322 biotoxin, domoic acid, J. Exp. Mar. Biol. Ecol. 382 (2010) 88-95.
- 323 [4] R.W.M. Kwong, W.-X. Wang, P.K.S. Lam, P.K.N. Yu, The uptake, distribution and  
324 elimination of paralytic shellfish toxins in mussels and fish exposed to toxic  
325 dinoflagellates, Aquat. Toxicol. 80 (2006) 82-91.
- 326 [5] V.M. Lopes, M. Baptista, T. Repolho, R. Rosa, P.R. Costa, Uptake, transfer and  
327 elimination kinetics of paralytic shellfish toxins in common octopus (*Octopus*  
328 *vulgaris*), Aquat. Toxicol. 146 (2014) 205-211.
- 329 [6] A.P. Sierra-Beltrán, A. Cruz, E. Núñez, L.M. Del Villar, J. Cerecero, J.L. Ochoa,  
330 An overview of the marine food poisoning in Mexico, Toxicon 36 (1998)  
331 1493-1502.
- 332 [7] A. Furey, S. O'Doherty, K. O'Callaghan, M. Lehane, K.J. James, Azaspiracid  
333 poisoning (AZP) toxins in shellfish: Toxicological and health considerations,  
334 Toxicon 56 (2010) 173-190.

- 335 [8] L.E. Fleming, B. Kirkpatrick, L.C. Backer, C.J. Walsh, K. Nierenberg, J. Clark, A.  
336 Reich, J. Hollenbeck, J. Benson, Y.S. Cheng, J. Naar, R. Pierce, A.J. Bourdelais,  
337 W.M. Abraham, G. Kirkpatrick, J. Zaias, A. Wanner, E. Mendes, S. Shalat, P.  
338 Hoagland, W. Stephan, J. Bean, S. Watkins, T. Clarke, M. Byrne, D.G. Baden,  
339 Review of Florida red tide and human health effects, *Harmful Algae* 10 (2011)  
340 224-233.
- 341 [9] T. Torgersen, J. Aasen, T. Aune, Diarrhetic shellfish poisoning by okadaic acid  
342 esters from Brown crabs (*Cancer pagurus*) in Norway, *Toxicon* 46 (2005)  
343 572-578.
- 344 [10] E. Prassopoulou, P. Katikou, D. Georgantelis, A. Kyritsakis, Detection of okadaic  
345 acid and related esters in mussels during diarrhetic shellfish poisoning (DSP)  
346 episodes in Greece using the mouse bioassay, the PP2A inhibition assay and  
347 HPLC with fluorimetric detection, *Toxicon* 53 (2009) 214-227.
- 348 [11] A. Li, J. Ma, J. Cao, P. McCarron, Toxins in mussels (*Mytilus galloprovincialis*)  
349 associated with diarrhetic shellfish poisoning episodes in China, *Toxicon* 60  
350 (2012) 420-425.
- 351 [12] A. Li, G. Sun, J. Qiu, L. Fan, Lipophilic shellfish toxins in *Dinophysis caudata*  
352 picked cells and in shellfish from the East China Sea, *Environ. Sci. Pollut. Res.*  
353 xxx (2014) xxx. Doi: 10.1007/s11356-014-3595-z
- 354 [13] S. Cordier, C. Monfort, L. Miossec, S. Richardson, C. Belin, Ecological analysis  
355 of digestive cancer mortality related to contamination by diarrhetic shellfish  
356 poisoning toxins along the coasts of France, *Environ. Res.* 84 (2000) 145-150.

- 357 [14] E. Manerio, V.L. Rodas, E. Costas, J.M. Hernandez, Shellfish consumption: A  
358 major risk factor for colorectal cancer, *Med. Hypotheses* 70 (2008) 409-412.
- 359 [15] L. MacKenzie, V. Beuzenberg, P. Holland, P. McNabb, A. Selwood, Solid phase  
360 adsorption toxin tracking (SPATT): a new monitoring tool that simulates the  
361 biotoxin contamination of filter feeding bivalves, *Toxicon* 44 (2004) 901-918.
- 362 [16] E. Fux, C. Marcaillou, F. Mondeguer, R. Bire, P. Hess, Field and mesocosm trials  
363 on passive sampling for the study of adsorption and desorption behaviour of  
364 lipophilic toxins with a focus on OA and DTX1, *Harmful Algae* 7 (2008)  
365 574-583.
- 366 [17] E. Fux, R. Bire, P. Hess, Comparative accumulation and composition of  
367 lipophilic marine biotoxins in passive samplers and in mussels (*M. edulis*) on the  
368 West Coast of Ireland, *Harmful Algae* 8 (2009) 523-537.
- 369 [18] T. Rundberget, E. Gustad, I.A. Samdal, M. Sandvik, C.O. Miles, A convenient  
370 and cost-effective method for monitoring marine algal toxins with passive  
371 samplers, *Toxicon* 53 (2009) 543-550.
- 372 [19] P. Rodríguez, A. Alfonso, E. Turrell, J.-P.Lacaze, L.M. Botana, Study of solid  
373 phase adsorption of paralytic shellfish poisoning toxins (PSP) onto different  
374 resins, *Harmful Algae* 10 (2011) 447-455.
- 375 [20] A. Caillaud, P. de la Iglesia, E. Barber, H. Eixarch, N. Mohammad-Noor, T.  
376 Yasumoto, J. Diogène, Monitoring of dissolved ciguatoxin and maitotoxin using  
377 solid-phase adsorption toxin tracking devices: Application to *Gambierdiscus*  
378 *pacificus* culture, *Harmful Algae* 10 (2011) 433-446.

- 379 [21] L.A. MacKenzie, *In situ* passive solid-phase adsorption of micro-algal biotoxins  
380 as a monitoring tool, *Curr. Opin. Biotech.* 21 (2010) 326-331.
- 381 [22] A. Li, F. Ma, X. Song, R. Yu, Dynamic adsorption of diarrhetic shellfish  
382 poisoning (DSP) toxins in passive sampling relates to pore size distribution of  
383 aromatic adsorbent, *J. Chromatogr. A* 1218 (2011) 1437-1442.
- 384 [23] H. Zhao, J. Qiu, H. Fan, A. Li, Mechanism and application of solid phase  
385 adsorption toxin tracking for monitoring microcystins, *J. Chromatogr. A* 1300  
386 (2013) 159-164.
- 387 [24] Z. Zendong, C. Herrenknecht, E. Abadie, C. Brissard, C. Tixier, F. Mondeguer, V.  
388 Séchet, Z. Amzil, P. Hess, Extended evaluation of polymeric and lipophilic  
389 sorbents for passive sampling of marine toxins, *Toxicon* xxx (2014) xxx. Doi:  
390 10.1016/j.toxicon.2014.03.010
- 391 [25] G. Pizarro, A. Moroño, B. Paz, J.M. Franco, Y. Pazos, B. Reguera, Evaluation of  
392 passive samplers as a monitoring tool for early warning of *Dinophysis* toxins in  
393 shellfish, *Mar. Drugs* 11 (2013) 3823-3845.
- 394 [26] Q. Gao, C. Pan, F. Liu, F. Lu, D. Wang, J. Zhang, Y. Zhu, Adsorption  
395 characteristics of malic acid from aqueous solutions by weakly basic  
396 ion-exchange chromatography, *J. Chromatogr. A* 1251 (2012) 148-153.
- 397 [27] X. Li, Z. Li, J. Chen, Q. Shi, R. Zhang, S. Wang, X. Wang, Detection, occurrence  
398 and monthly variations of typical lipophilic marine toxins associated with  
399 diarrhetic shellfish poisoning in the coastal seawater of Qingdao City, China,  
400 *Chemosphere* 111 (2014) 560-567.

403 **Table1** Dynamic adsorption equations for OA and DTX1 toxins by HP20 resin simulated using different mathematical models.

Salinity of seawater	Toxins	Elovich equation $q=a+b \times \ln t$	Double constant equation $\ln q=b \times \ln t+\ln a$	Parabolic diffusion equation $q=a+b \times \sqrt{t}$	First order kinetic equation $\ln q=a+b \times t$	Pseudo-secondary kinetics equation $t/q=a+b \times t$
High salinity (27‰)	OA	$y=134.8 x-306.1$ $R^2=0.9199$	$y=0.558x+3.43$ $R^2=0.9215$	$y=38.62 x+31.46$ $R^2=0.8993$	$y=0.0158x+4.16$ $R^2=0.9588$	$y=0.00091x+0.1153$ $R^2=0.9776$
	DTX1	$y=333.5x-790.1$ $R^2=0.9502$	$y=0.684 x+3.28$ $R^2=0.9517$	$y=56.74 x+40.54$ $R^2=0.8923$	$y=0.0043x+5.61$ $R^2=0.5324$	$y=0.00062x+0.0816$ $R^2=0.9832$
Medium salinity (13.5‰)	OA	$y=116.2 x-166.5$ $R^2=0.9474$	$y=0.449x+4.29$ $R^2=0.9305$	$y=44.51 x+106.73$ $R^2=0.8816$	$y=0.0027x+5.84$ $R^2=0.5225$	$y=0.00098x+0.0534$ $R^2=0.9957$
	DTX1	$y=302.2 x-488.3$ $R^2=0.9597$	$y=0.438 x+4.70$ $R^2=0.9371$	$y=63.45 x+153.12$ $R^2=0.8858$	$y=0.0027x+6.20$ $R^2=0.5452$	$y=0.00069x+0.0374$ $R^2=0.9951$
Low salinity (9‰)	OA	$y=99.1 x-125.0$ $R^2=0.9573$	$y=0.329 x+4.20$ $R^2=0.9476$	$y=31.97 x+139.03$ $R^2=0.8995$	$y=0.0083x+4.97$ $R^2=0.9440$	$y=0.0011x+0.0668$ $R^2=0.9964$
	DTX1	$y=263.1x-406.5$ $R^2=0.9761$	$y=0.383x+4.81$ $R^2=0.9456$	$y=48.06 x+195.47$ $R^2=0.8963$	$y=0.0027x+6.10$ $R^2=0.6148$	$y=0.00072x+0.0454$ $R^2=0.9979$

404

405 **Table2** Comparison of experimental values and theoretical values of adsorption of OA  
 406 and DTX1 toxins by HP20 resin simulated by the Pseudo-secondary kinetics equation.

Salinity of seawater	Toxins	Pseudo-secondary kinetics equation	$h$	$Q_{e,cal}$	$Q_{e,exp}$
<b>High salinity</b> (27‰)	OA	$y=0.00091x+0.1153$	8.67	1100	901
	DTX1	$y=0.00062x+0.0816$	12.25	1610	1310
<b>Medium salinity</b> (13.5‰)	OA	$y=0.00098x+0.0534$	18.73	1020	900
	DTX1	$y=0.00069x+0.0374$	26.74	1450	1290
<b>Low salinity</b> (9‰)	OA	$y=0.0011x+0.0668$	14.97	909	868
	DTX1	$y=0.00072x+0.0454$	22.03	1390	1280

407 Note:  $h(=1/a)$  means the initial sorption rate (ng/(g·min));  $Q_{e,cal}(=1/b)$  means the  
 408 theoretical values were calculated according to the Pseudo-secondary kinetics  
 409 equations;  $Q_{e,exp}$  means the actual values were tested in the adsorption experiments.

410

411 **Table3** Specific surface areas and average pore volumes of HP20 resins before and  
 412 after adsorption for OA and DTX1 toxins in seawaters of different salinity.

Salinity of seawaters	Characteristic index	Before adsorption for toxins	After adsorption for toxins	Changing ratio (%)
<b>High salinity (27‰)</b>	Specific surface area (m <sup>2</sup> /g)	654.7	539.3	-17.6
	Average pore volume (cm <sup>3</sup> /g)	1.30	1.18	-9.2
<b>Medium salinity (13.5‰)</b>	Specific surface area (m <sup>2</sup> /g)	558.3	546.0	-2.2
	Average pore volume (cm <sup>3</sup> /g)	1.01	1.18	+16.8
<b>Low salinity (9‰)</b>	Specific surface area (m <sup>2</sup> /g)	604.5	552.3	-8.6
	Average pore volume (cm <sup>3</sup> /g)	1.11	0.97	-12.6

413 Note: specific surface area was calculated by the BET model; average pore volume  
 414 (pore size 1.7 - 300 nm) was calculated by the BJH model.

415 **Legends of figures**

416 Fig.1. Chemical structures of OA and its analogue DTX1.

417 Fig.2. LC-MS/MS chromatograms of OA and DTX1 in one sample collected from the  
418 artificial seawater at low salinity after 30-min exposure in adsorption experiment.

419 Three different transitions of parent ions  $m/z$  827.5 and 841.5 were used to  
420 qualify OA and DTX1, respectively. The concentrations of OA and DTX1 in this  
421 sample were tested as 1.85 and 2.77 ng/mL, respectively.

422 Fig.3. Dynamic adsorption curves of OA (a) and DTX1 (b) toxins by HP20 resin in  
423 seawaters with different salinity.

424 Fig.4. Average linear adsorption rates of OA (a) and DTX1 (b) toxins by HP20 resin  
425 in seawaters with different salinity calculated in different time period.

426 Fig.5. Accumulative pore volumes for different interval pore size of HP20 resin  
427 before and after adsorption for OA and DTX1 toxins in seawaters with different  
428 salinity.

429 Fig.6. Scanning electron microscopes (SEM) of HP20 resin before and after  
430 adsorption under different salinity conditions. SEM of high salinity blank (a) and  
431 high salinity (b), medium salinity blank (c) and medium salinity (d), low salinity  
432 blank (e) and low salinity (f) are compared separately.

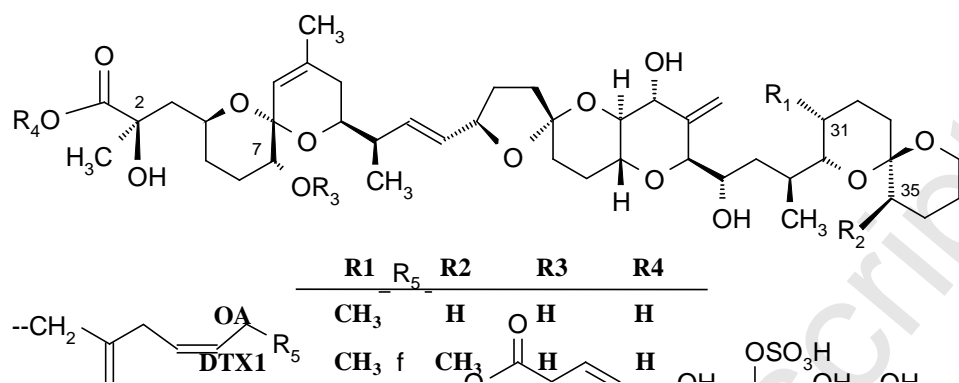
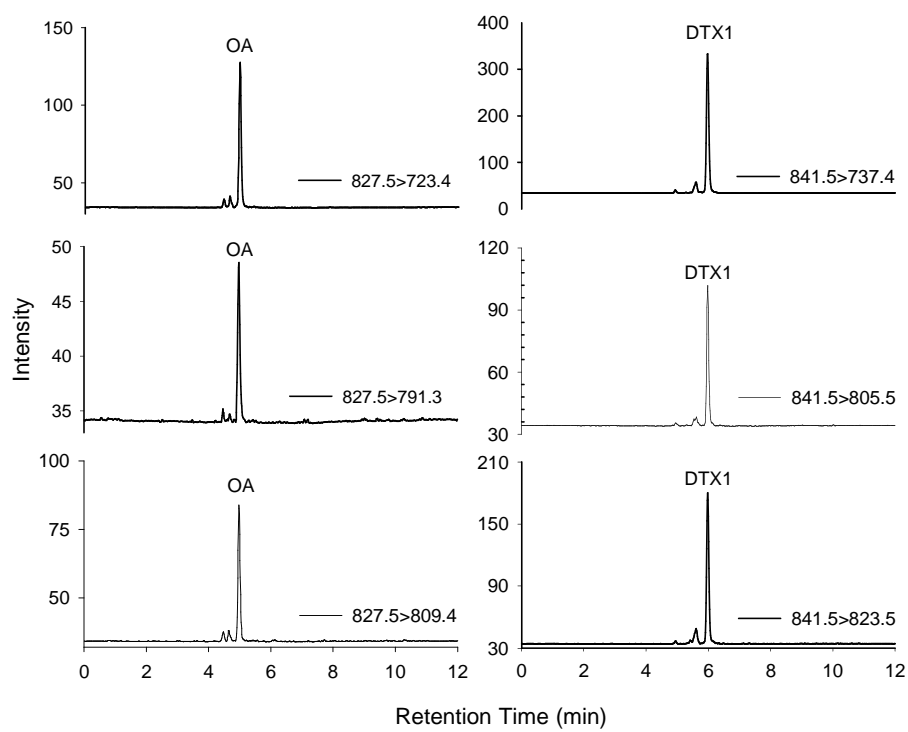
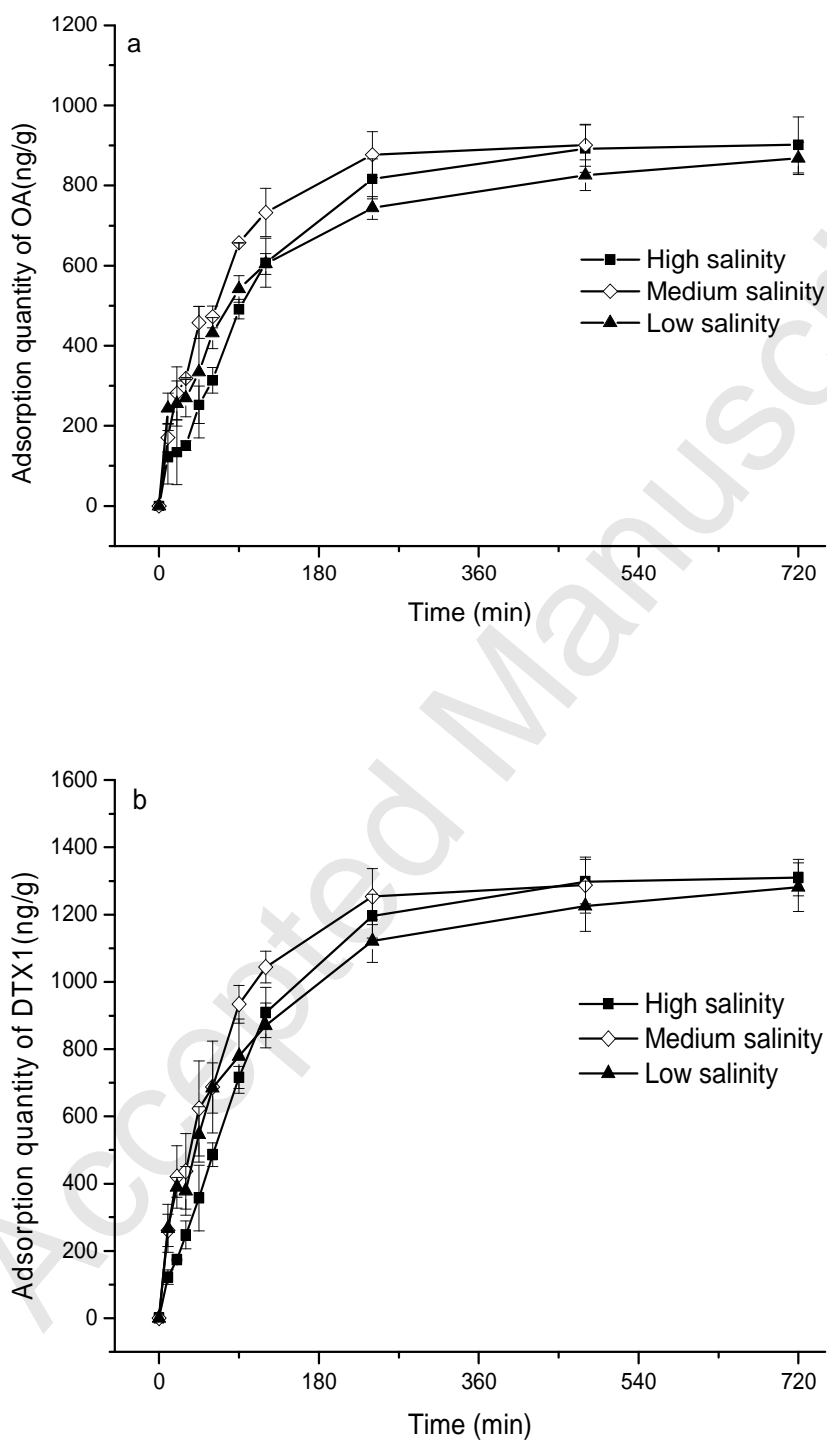
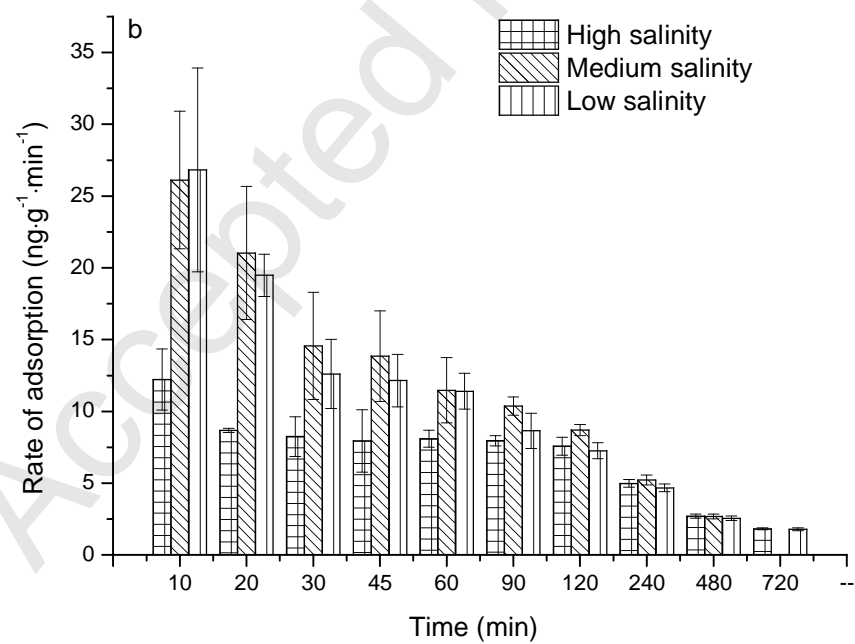
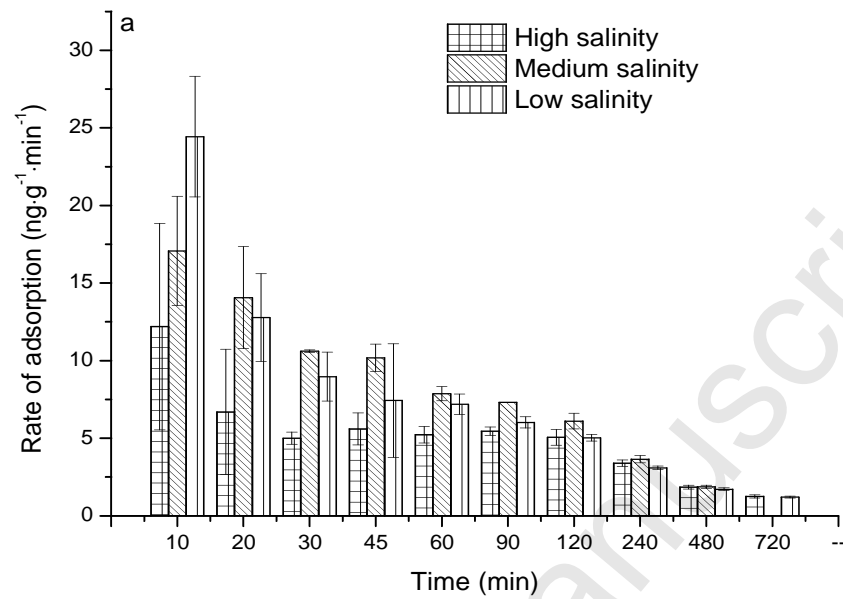
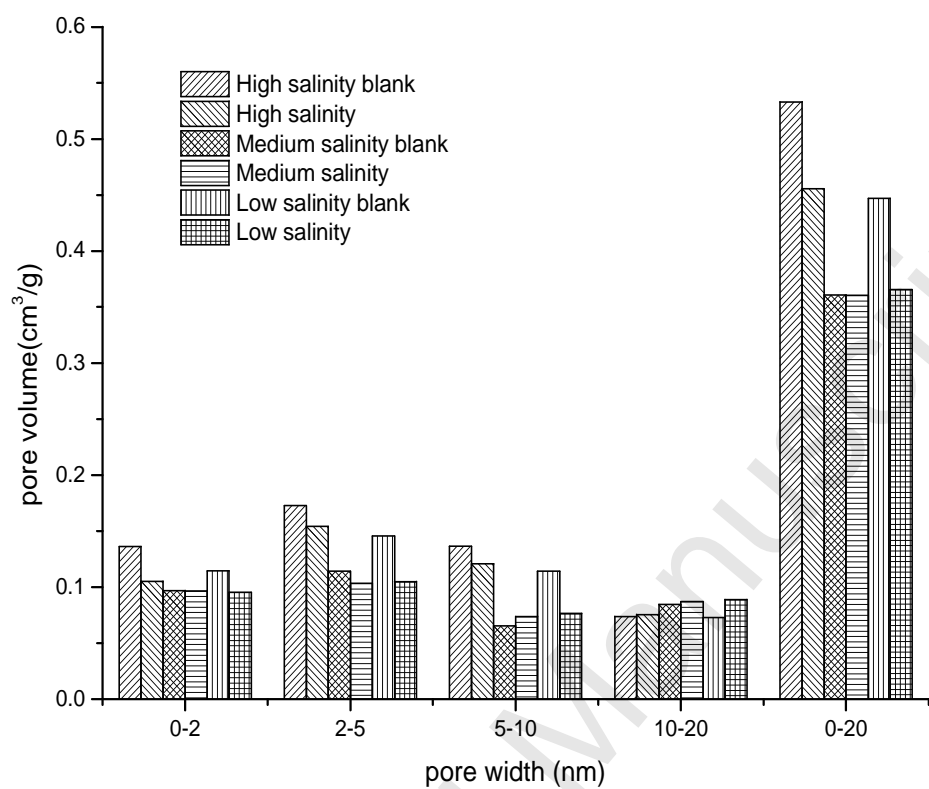


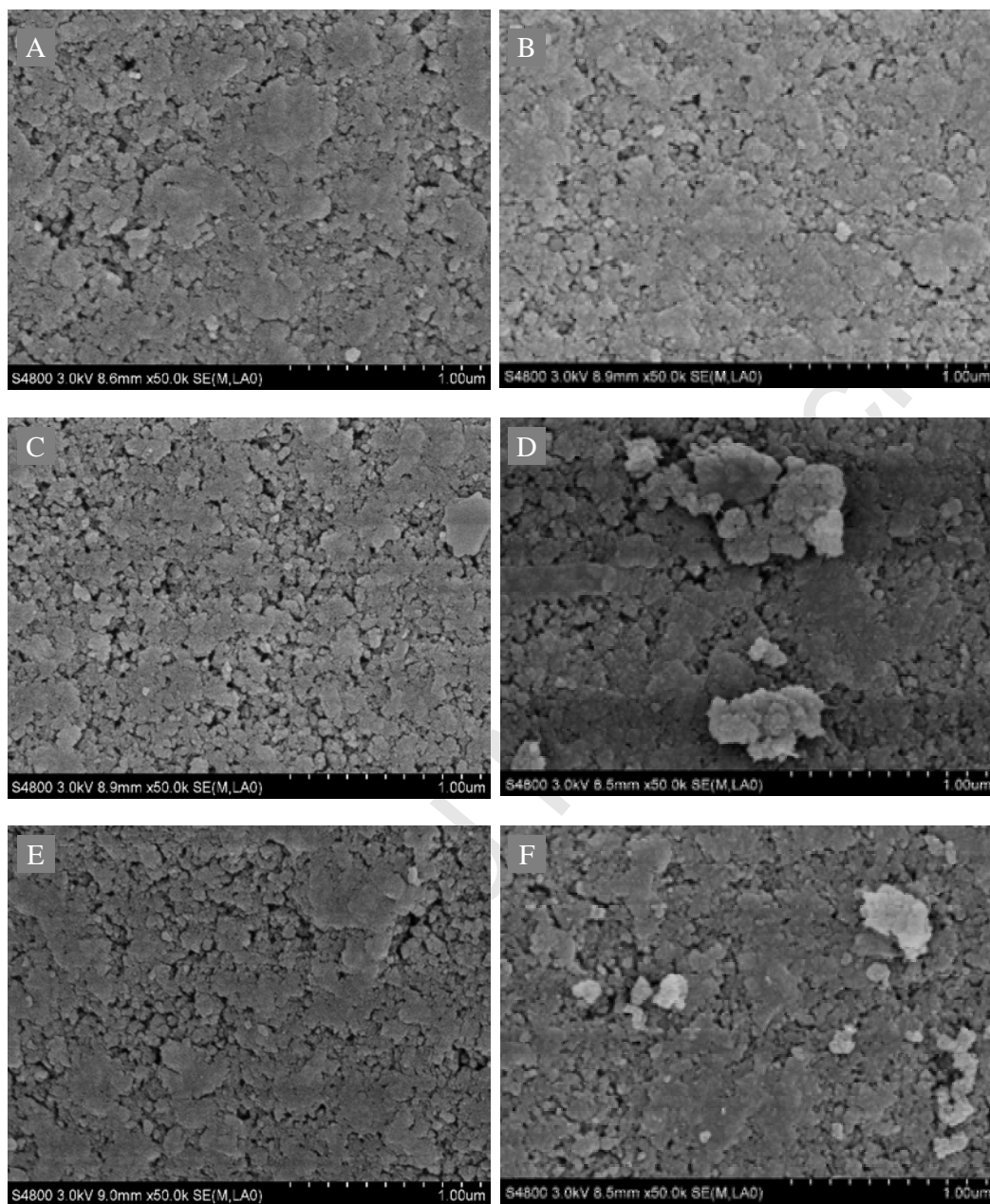
Fig. 1

**Fig.2**

**Fig. 3**

**Fig. 4**

**Fig. 5**

**Fig. 6**